Maltol inhibits oxygen glucose deprivation-induced chromatinolysis in SH-SY5Y cells by maintaining pyruvate level

SHUYAN ZHANG[1], XINYUE ZHANG[2], XUANZHONG WANG[3,4], CHEN LI[3,4], CHUAN HE[1,4], TIANFEI LUO[4,5] and PENGFEI GE[3,4]

[1]Department of Neurotrauma, First Hospital of Jilin University, Changchun, Jilin 130021, P.R. China; [2]Department of Public Health, New York University, New York, NY 10016, USA; [3]Department of Neurosurgery; [4]Research Center of Neuroscience; [5]Department of Neurology, First Hospital of Jilin University, Changchun, Jilin 130021, P.R. China

Received August 11, 2022; Accepted January 25, 2023

DOI: 10.3892/mmr.2023.12962

Abstract. Maltol, a chemical isolated from ginseng root, has shown treatment effects on several pathological processes including osteoarthritis, diabetic peripheral neuropathy and liver fibrosis. Nevertheless, its effect on ischemia-induced neuron death remains elusive. In the present study, the treatment effect of maltol on ischemia-induced neuron damage was investigated by using oxygen and glucose deprivation (OGD) model in SH-SY5Y cells. *In vitro* studies revealed that maltol protected SH-SY5Y cells against OGD-induced chromatinolysis by inhibiting two reactive oxygen species (ROS)-regulated pathways. One was DNA double-strand breaks and the other was nuclear translocation of apoptosis inducing factor. Mechanistically, maltol not only inhibited OGD-induced depletion of glutathione and cysteine by maintaining cystine/glutamate antiporter (xCT) level, but also abrogated OGD-induced catalase downregulation. Meanwhile, maltol also alleviated OGD-induced inactivation of mTOR by attenuating OGD-induced depletion of adenosine triphosphate and pyruvate and downregulation of pyruvate kinase M2, indicating that maltol inhibited the glycolysis dysfunction caused by OGD. Considering that activated mammalian target of the rapamycin (mTOR) could lead to enhanced xCT expression and decreased catalase degradation by autophagy, these findings indicated that maltol attenuated OGD-induced ROS via inhibition of mTOR inactivation by maintaining pyruvate level. Taken together, it was demonstrated that maltol prevented OGD-induced chromatinolysis in SH-SY5Y cells via inhibiting pyruvate depletion.

Correspondence to: Professor Pengfei Ge, Department of Neurosurgery, First Hospital of Jilin University, 1 Xinmin Avenue, Changchun, Jilin 130021, P.R. China
E-mail: gepf@jlu.edu.cn

Key words: oxygen glucose deprivation, maltol, chromatinolysis, glycolysis, apoptosis inducing factor

Introduction

All the necessary information of maintaining cellular physiological functions is contained in nuclear DNA, which is an essential macromolecule in eukaryotic cells (1). Enzymatic degradation of nuclear DNA is defined as chromatinolysis (2), which plays dual roles in regulating cellular destiny. On one hand, degradation of damaged DNA could prevent genetic mutations and disease occurrence. On the other hand, excessive chromatinolysis facilitates disassembly of nucleus and makes cell death irreversible. The mechanisms accounting for chromatinolysis remain elusive, but previous studies have shown that gamma H2A histone family member X (γ-H2AX) formation and nuclear translocation of apoptosis inducing factor (AIF) are two crucial factors leading to chromatinolysis (2,3). γ-H2AX often forms at the breaking location of DNA double strands and serves as a platform recruiting nucleases (4). AIF is a protein located within the space between mitochondrial inner and outer membranes. After translocating into nucleus and being recruited to γ-H2AX, it could degrade DNA into oligonucleotides or smaller molecules (2). Several compounds have been shown to eliminate cancer cells via inducing chromatinolysis (5-7), but it remains elusive whether chromatinolysis is involved in regulation of ischemia-induced neuronal death.

Maltol (3-hydroxy-2-methyl-4-pyrone) is a chemical isolated from ginseng root via Maillard reaction (8). Although being widely used as a food flavoring agent, it has multiple bio-activities including anti-oxidative stress, anti-inflammatory and anti-apoptotic (9-11). Moreover, it effectively inhibits several pathological processes including osteoarthritis, diabetic peripheral neuropathy and liver fibrosis (12-14). In mice, maltol has neuroprotective effects against hypoxia-induced damage in neurons (15,16). Similarly, it could also inhibit neuronal death after spinal cord injury by inhibiting oxidative stress (17). These results indicated a potential neuroprotective effect of maltol against ischemia-induced neuronal damage. A major factor leading to the neuron death caused by cerebral ischemia, traumatic brain injury and epilepsy is oxygen and glucose deprivation (OGD) (18), which is often used to investigate the effects of natural chemicals on neuronal damage.

SH-SY5Y cells are human neuroblastoma cells with similar properties with neurons in electrophysiology, neurochemistry and morphology. For this reason, SH-SY5Y cells stressed by OGD are often used as an *in vitro* model to investigate neuronal injury or death caused by ischemic insults (19). In the present study, the effect of maltol on neuronal damage caused by ischemia was investigated using the OGD model in SH-SY5Y cells.

Materials and methods

Reagents. Maltol and pyruvate sodium were both purchased from MilliporeSigma. Primary antibodies against AIF (cat. no. ab32516), phosphorylated (p)-H2AX at S139 (cat. no. ab81299), ATM (cat. no. ab32420), p-ATM at S1981 (cat. no. 81292), catalase (cat. no. ab209211), cystine/glutamate antiporter (xCT) (cat. no. ab175186), mTOR (cat. no. ab134903), p-mTOR (cat. no. 109268), PKM2 (cat. no. ab89364), p-JNK (cat. no. ab124956), TOMM20 (cat. no. ab186735) and H2A (cat. no. ab177308) were all obtained from Abcam. Primary antibody against β-actin was obtained from Cell Signaling Technology, Inc.

Cell line and culture and cellular viability assay. SH-SY5Y cells were obtained from Shanghai institute of cell biology, Chinese Academy of Sciences (Shanghai, China). The cells were authenticated by STR profiling. Cells were cultured in DMEM medium (Hyclone; Cytiva) with high glucose supplemented with 10% FBS (Clark Bioscience), penicillin (100 U/ml) and streptomycin (100 μg/ml), and maintained at 37˚C and 5% CO_2 in a humid environment. MTT assay kit was used for cellular viability examination and DMSO was used to dissolve the purple formazan. The results were expressed as a ratio of the absorbance at 570 nm to that in control cells.

Assay of intracellular GSH and cysteine. The intracellular GSH levels were assayed by using GSH assay kit (cat. no. S0052; Beyotime Institute of Biotechnology) following the manufacturer's protocol. The result was displayed as a ratio of the absorbance of each prepared sample at 412 nm to that of control cells.

The intracellular cysteine levels were determined by cysteine assay kit (cat. no. A126-1-1; Nanjing Jiancheng Bioengineering Institute) according to the manufacturer's instructions. The result was expressed as a ratio of the absorbance of each prepared sample at 600 nm to that of control cells.

Measurement of reactive oxygen species (ROS). Intracellular ROS levels were detected by using DCFH-DA, which was obtained from Beyotime Institute of Biotechnology. The operation protocol was conducted according to the manufacturer. Fluorescence was measured using a fluorescence spectrometer (HTS 7000; PerkinElmer, Inc.) at an excitation wavelength of 485 nm and an emission wavelength of 530 nm. The ROS levels were displayed as arbitrary unit/mg protein, then as a ratio to control. A fluorescence microscope (IX71; Olympus Corporation) was used to observe and image the cells seeded on six-well plates stained with DCFH-DA.

Neutral comet assay. Neutral comet assay was performed as previously described (20). Briefly, SH-SY5Y cells with or without OGD treatment were collected and suspended in low-melting agarose. After deposited on comet slides pre-layered with regular-melting agarose, the cells were covered with coverslips and cooled down at 4˚C for 10 min. Afterwards, the cells were lysed in darkness at 4˚C for 1 h and washed for 10 min in TBE buffer. After electrophoresed and washed, the cells were neutralized and stained with acridine orange for 5 min.

The slides were observed and images were captured by using a fluorescence microscope (IX71; Olympus Corporation). ImageJ software v1.54 (National Institutes of Health) and OpenComet 1.3 software (National Institutes of Health) were applied to measure the cell number with DNA comets and the DNA percent content in comet tail region (four assays, each with ~100 cells analyzed).

Gel electrophoresis and western blotting. SH-SY5Y cells were collected and homogenized as previously described (20). The homogenates were centrifuged to isolate cytoplasmic, mitochondria and nuclear fractions (21). The protein content in each fraction was assayed with a BCA Protein assay kit (Beyotime Institute of Biotechnology). Equal quantities of protein (30 μg per lane) were electrophoresed on 8-12% sodium dodecyl sulfate-polyacrylamide gels based on the molecular weight of the target protein and transferred to PVDF membranes. The membranes were then blocked with 5% skimmed milk in PBS for 2 h at room temperature and incubated overnight at 4˚C with primary antibodies. Then, the membrane was incubated with horseradish peroxidase-conjugated secondary antibody at room temperature for 2 h and washed with PBS for three times. All the primary antibodies and secondary antibodies were diluted with PBS-T (0.05% Tween-20) at 1:1,000. Eventually, immunoreactive proteins were visualized by using a chemiluminescence developer (ChemiScope 5300; Clinx Science Instrument Co., Ltd.). The loading controls in western blotting used in the present study were as follows: β-actin was used for cytoplasm fraction (22), Tomm20 was used for mitochondrial fraction (23) and H2AX was used for nuclear fraction (6).

Immunocytochemical staining. The SH-SY5Y cells ($8x10^4$ cells/well) were seeded on a culture dish. After OGD, they were fixed in ethanol, washed with PBS, and incubated with 1% Triton X-100 for 10 min at 4˚C. After blocking the non-specific antibody binding sites with 5% skimmed milk in PBS for 2 h at room temperature, the cells were incubated overnight with anti-γ-H2AX (1:100; cat. no. ab81299; Abcam) or anti-AIF (1:100; cat. no. ab32516; Abcam) followed by incubation in Alexa Fluor 488-conjugated or Alexa Fluor 647-conjugated goat anti-rabbit IgG (1:200; cat. nos. A0423 or A0468; Beyotime Institute of Biotechnology) for 1 h and then with Heochst33258. Finally, all the cells were observed under laser scanning confocal microscope (FV1000; Olympus Corporation).

Mitochondrial membrane potential assay. The cells were collected and stained with JC-1 at 37˚C for 20 min according to the manufacturer's instruction (Beyotime Institute of Biotechnology). After washed with PBS, the cells were assayed by flow cytometry (FACScan) and analyzed using CELLquest pro software 5.1 (both from Becton-Dickinson and Company)

observed under fluorescence microscope (IX71; Olympus Corporation).

Statistical analyses. All data was acquired from at least four independent experiments and are expressed as the mean ± standard deviation. Statistical analyses were performed with Microsoft Excel 2010 (Microsoft Corporation) and GraphPad Prism 6 software (GraphPad Software, Inc.). Statistical comparisons were made using one-way ANOVA with Tukey's post hoc test. $P<0.05$ was considered to indicate a statistically significant difference.

Results

Maltol inhibits OGD-induced death and chromatinolysis in SH-SY5Y cells. To investigate whether maltol has protective effect on neurons stressed with OGD, MTT assay was used to examine cellular viabilities. As previously described (24), SH-SY5Y cells were pretreated 1 h with maltol at 0.5, 1.0, 2.0 and 4.0 mmol/l and then stressed with OGD for 24 h. As revealed in Fig. 1A, the viability of the SH-SY5Y cells was decreased by OGD significantly when compared with that of control cells. Light microscopy showed that the control cells were polygonal, but majority of the cells stressed with OGD became smaller and round (Fig. 1B). By contrast, OGD-induced reduction in cellular viability was apparently prevented in the cells pretreated with 0.5 mmol/l maltol, and further prevented when maltol dosage was increased to 1.0 mmol/l (Fig. 1A). Pretreatment of maltol at 4 mmol/l alone could inhibit cellular viabilities, and the effect of maltol at 2 mmol/l was less significant than that of maltol at 0.5 and 1.0 mmol/l (Fig. 1A). Thus, maltol at 0.5 and 1 mmol/l was used in the subsequent studies. Morphologically, the cells with smaller size and round shape caused by OGD were obviously inhibited in the presence of maltol (Fig. 1B). Therefore, the aforementioned results indicated that maltol could effectively prevent OGD-induced injury in SH-SY5Y cells.

To clarify why maltol could exert protection against OGD-induced damage, agarose gel electrophoresis was used to assay its effect on chromatinolysis because chromatinolysis is a final event leading to cell death (1). In comparison with control cells, the DNA isolated from OGD-stressed cells presented smear band on agarose gel after being subjected to electrophoresis, which was obviously inhibited in the cells pretreated with 0.5 mmol/l maltol (Fig. 1C). Notably, the inhibitory effect of 1.0 mmol/l maltol was more obvious than that produced by 0.5 mmol/l maltol. This suggested that maltol protects SH-SY5Y cells against OGD-induced damage via inhibiting chromatinolysis in a dose-dependent manner.

Maltol inhibits OGD-induced nuclear translocation of AIF via inhibition of JNK activation. AIF that is located at mitochondria could serve as a nuclease after translocation into nuclei and being recruited to γ-H2AX; therefore, western blotting was used to analyze the effect of OGD on AIF distribution. Compared with control cells, mitochondrial AIF was apparently decreased by OGD, whereas nuclear AIF was increased correspondingly (Fig. 1E). Consistently, confocal microscopy revealed that AIF accumulated obviously in the nuclei of OGD-stressed cells (Fig. 1D). This indicated that OGD induced AIF translocation from mitochondria to nuclei. Given that AIF release from mitochondria is decided by mitochondrial depolarization (25), JC-1 staining combined with flow cytometry was used to examine OGD-induced changes in mitochondrial membrane potentials. JC-1 displays high red fluorescence after accumulation in mitochondria, but it exists in the cytoplasm and emits green fluorescence when the mitochondrial membrane potential is exhausted. Both fluorescence microcopy and flow cytometry revealed that red fluorescence decreased obviously in the cells stressed with OGD, when compared with control cells (Fig. 1F and G). It has been reported that activated JNK could aggravate cerebral ischemia-induced mitochondrial depolarization by translocation to mitochondria (26). The effect of OGD on p-JNK distribution was examined using western blotting. Compared with control cells, cytoplastic and mitochondrial p-JNK were obviously increased by OGD (Fig. 1E and F). These findings indicated that OGD induced mitochondrial depolarization in SH-SY5Y cells. By contrast, OGD-induced depletion of mitochondrial membrane potential, translocation of AIF from mitochondria to nuclei as well as increased p-JNK in mitochondria were all inhibited by maltol (Fig. 1E-H). Therefore, these data indicated that maltol inhibited OGD-induced nuclear translocation of AIF.

Maltol inhibits OGD-induced DNA double-strand breaks (DSBs) in SH-SY5Y cells. To elucidate why maltol could inhibit chromatinolysis, neutral comet assay was used to examine its effect on DNA DSBs that is a crucial step leading to chromatinolysis. When compared with control cells, the majority of the cells stressed with OGD presented long comet tails (Fig. 2A). Statistical analysis proved that the cells with comet tails and the DNA content in the tails were both significantly improved by OGD (Fig. 2B and C). Moreover, confocal microscopy showed that γ-H2AX foci, a prominent biomarker of DNA DSBs, formed extensively in the nuclei of OGD-stressed cells (Fig. 2D). Furthermore, western blot analysis revealed that the protein level of γ-H2AX was upregulated by OGD, when compared with control cells (Fig. 2E). Consistently, p-ATM accounting for γ-H2AX formation was also upregulated by OGD at each indicated time, although the ratio of p-ATM/ATM presented no statistical difference (Fig. 2E and F). These results indicated the OGD-induced DNA DSBs in SH-SY5Y cells. By contrast, pretreatment with 1.0 mmol/l maltol obviously inhibited OGD-induced increase in cells with comet tails and improvement of DNA content in comet tails (Fig. 2A-C). Notably, maltol obviously attenuated OGD-induced upregulation of γ-H2AX and p-ATM in a dose-dependent manner (Fig. 2E). Therefore, these data indicated that maltol inhibited OGD-induced DNA DSBs.

Maltol inhibits OGD-induced ROS via maintaining catalase, xCT, GSH and cysteine levels. Because oxidative stress characterized by intracellular accumulation of ROS is a factor leading to nuclear translocation of AIF and DNA DSBs and OGD could induce oxidative stress (6,24), DCFH-DA (a probe for ROS) was used to examine whether maltol could inhibit OGD-induced ROS. As revealed by fluorescence microscopy, the green fluorescence exhibited by DCFH-DA was markedly brighter in OGD-stressed cells

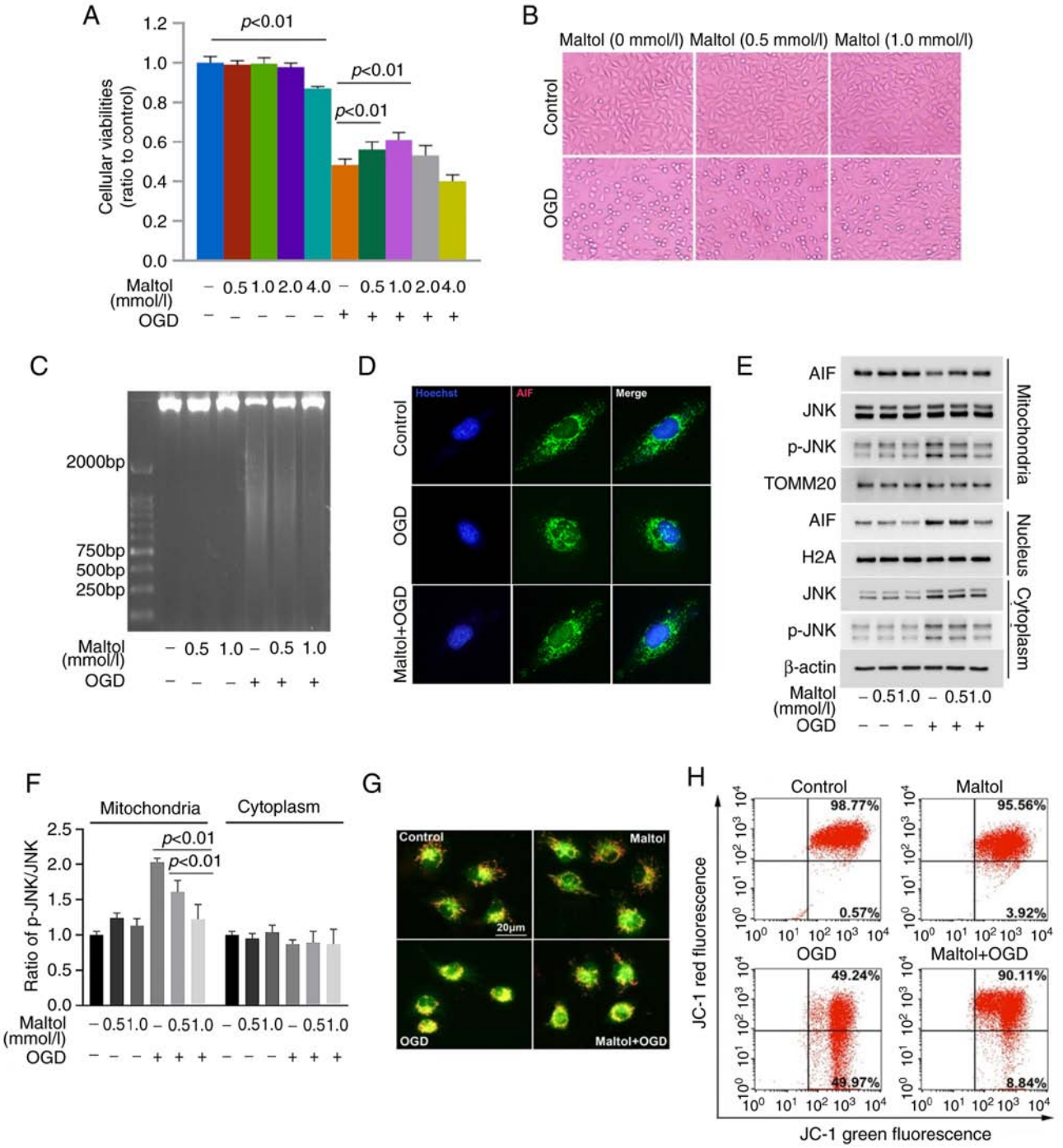

Figure 1. Maltol prevents OGD-induced chromatinolysis and mitochondrial damage. (A) MTT assay revealed that OGD-induced decrease in the viabilities of SH-SY5Y cells was significantly prevented by pretreatment with maltol at 0.5 and 1.0 mmol/l. Pretreatment of maltol at 4 mmol/l alone could decrease cellular viabilities, and the effect of maltol at 2 mmol/l was less significant than that of maltol at 0.5 and 1.0 mmol/l. (B) Light microscopy showed that majority of the cells stressed by OGD became smaller and round, which was obviously prevented by maltol. (C) The smear band exhibited by the nuclear DNA extracted from OGD-stressed cells on agarose gel was apparently inhibited by pretreatment with maltol. (D) Confocal microscopy with immunocytochemical staining revealed that OGD triggered AIF accumulation in nucleus, which could be inhibited in the presence of maltol. (E) Western blotting demonstrated that maltol prevented OGD-induced AIF downregulation in mitochondrial fraction and upregulation in nuclear fraction, as well as suppressed JNK activation and translocation to mitochondria. (F) Statistical analysis demonstrated that the ratio of p-JNK/JNK in mitochondria was obviously enhanced by OGD, which could be prevented by maltol. (G) Fluorescence microscopy in combination with JC-1 staining showed that OGD-induced reduction in red fluorescence was partially inhibited in the presence of maltol. (H) Flow cytometry combined with JC-1 staining identified that OGD-induced reduction in red fluorescence was inhibited by maltol. OGD, oxygen and glucose deprivation; AIF, apoptosis inducing factor; p-, phosphorylated.

than that in control cells, which was obviously attenuated in the cells pretreated with 1.0 mmol/l maltol (Fig. 3A). Statistical analysis proved as well that the increased fluorescence intensity caused by OGD could be significantly inhibited by 0.5 mmol/l maltol, and further inhibited when maltol dosage was improved to 1.0 mmol/l (Fig. 3B). These results indicated that maltol inhibited OGD-induced ROS in a dose-dependent manner.

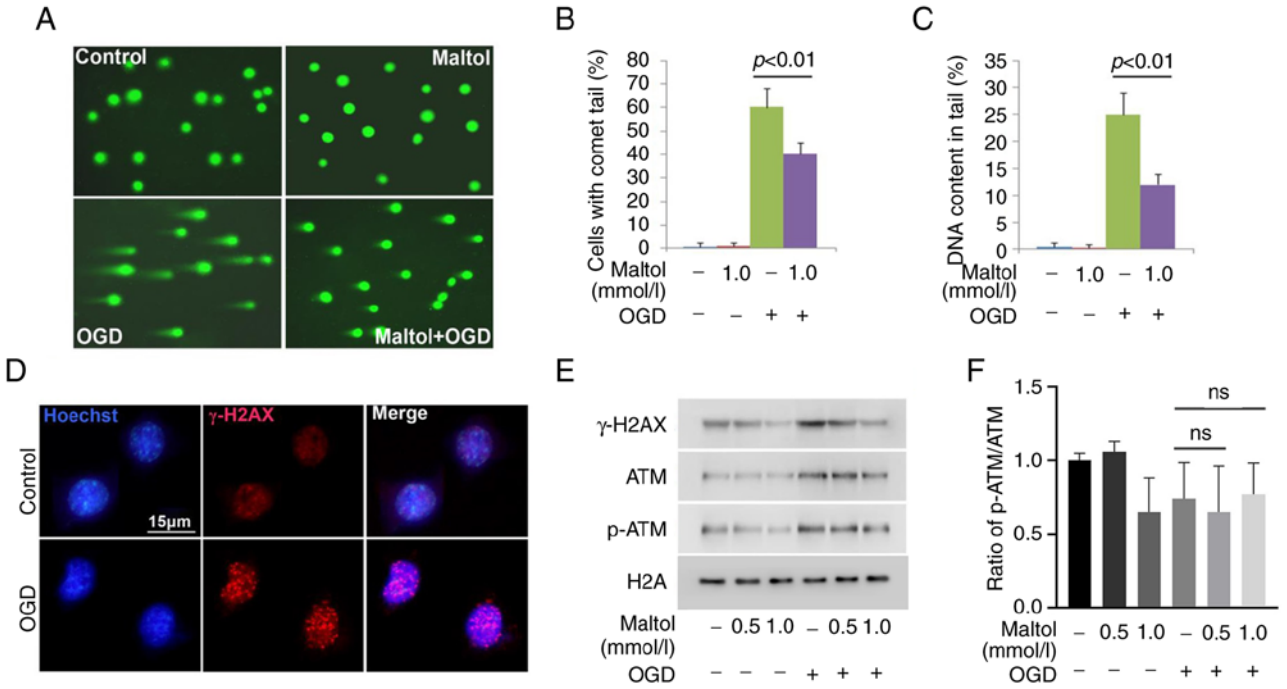

Figure 2. Maltol inhibits OGD-induced DNA double-strand breaks. (A) Neutral comet assay showed that maltol at 1.0 mmol/l apparently inhibited OGD-induced increase of the cells with comet tails. (B) Statistical analysis revealed that maltol effectively inhibited the cells with comet tails. (C) Statistical analysis revealed that maltol effectively inhibited the DNA content in the comet tails. (D) Confocal microscopy combined with immunocytochemical staining showed that OGD induced formation of numerous puncta in nucleus. (E) Western blotting proved that maltol obviously inhibited OGD-induced upregulation of λ-H2AX, ATM and p-ATM. (F) The statistical analysis demonstrated that there was no significant difference in the ratio of p-ATM/ATM in cells treated as indicated. OGD, oxygen and glucose deprivation; p-, phosphorylated; ns, no significance.

To address why maltol could prevent OGD-induced ROS, its effect was examined on catalase (which can catalyze reduction of hydrogen peroxide into water and oxygen) and GSH (an intracellular antioxidant synthesized from cysteine) (27). As revealed by western blotting, maltol exerted inhibitory effect on OGD-induced downregulation of catalase, which became more apparent when maltol dosage was increased from 0.5 to 1.0 mmol/l (Fig. 3C and D). Although GSH and cysteine were both depleted by OGD, their levels were maintained dose-dependently by maltol (Fig. 3E and F). Since cysteine is converted from cystine, the effect of maltol on the protein level of SLC7A11 was investigated. As a light chain of xCT accounting for transporting extracellular cystine into cells, SLC7A11 level is also regulated by activated mTOR (28). It was revealed that maltol inhibited OGD-induced downregulation of SLC7A11 and p-mTOR in a dose-dependent manner (Fig. 3C and D). Therefore, the aforementioned results indicated that maltol prevented OGD-induced ROS via inhibiting depletion of GSH and cysteine, downregulation of catalase and SLC7A11, and inactivation of mTOR.

Maltol inhibits OGD-induced mTOR inactivation by maintaining pyruvate level. To address why maltol prevented OGD-induced mTOR inactivation, its effect on OGD-induced changes in glycolysis function was investigated, considering that glycolysis dysfunction leads to mTOR inactivation (29). It was found that OGD induced obvious depletion of ATP and pyruvate (Fig. 4A and B). Moreover, western blotting showed as well that PKM2 was obviously downregulated by OGD (Fig. 4C). These indicated that OGD induced glycolysis dysfunction.

Given that pyruvate could be used to generate ATP after entering TCA (30), the SH-SY5Y cells were pretreated with exterior pyruvate at 10 mmol/l for 1 h and then stressed with OGD for 24 h. It was found that supplement of exterior pyruvate not only inhibited OGD-induced death in SH-SY5Y cells, but also reversed ATP depletion (Fig. 4D and F). Consistently, pyruvate apparently inhibited OGD-induced downregulation of p-mTOR (Fig. 4G and H). This indicated that pyruvate depletion exacerbated OGD-induced mTOR inactivation. Moreover, OGD-induced downregulation of xCT and depletion of cysteine and GSH were all prevented by pyruvate (Fig. 4G, I and J). The smear band on agarose gel presented by the DNA isolated from OGD-stressed cells was obviously inhibited by pyruvate (Fig. 4E). The aforementioned results indicated that pyruvate depletion contributed to OGD-induced mTOR inactivation.

Notably, it was revealed that the depleted pyruvate and ATP and downregulated PKM2 caused by OGD were all prevented by maltol in a dose-dependent manner (Fig. 4A-C). These indicated that maltol inhibited pyruvate depletion caused by OGD by maintaining glycolysis function.

Discussion

In summary, it was demonstrated in the present study that maltol protected SH-SY5Y cells against OGD-induced chromatinolysis by inhibiting DNA DSBs and nuclear translocation of AIF. Then, it was found that maltol attenuated OGD-induced ROS, which could lead to DNA DSBs and nuclear translocation of AIF. Mechanistically, it was revealed that maltol attenuated

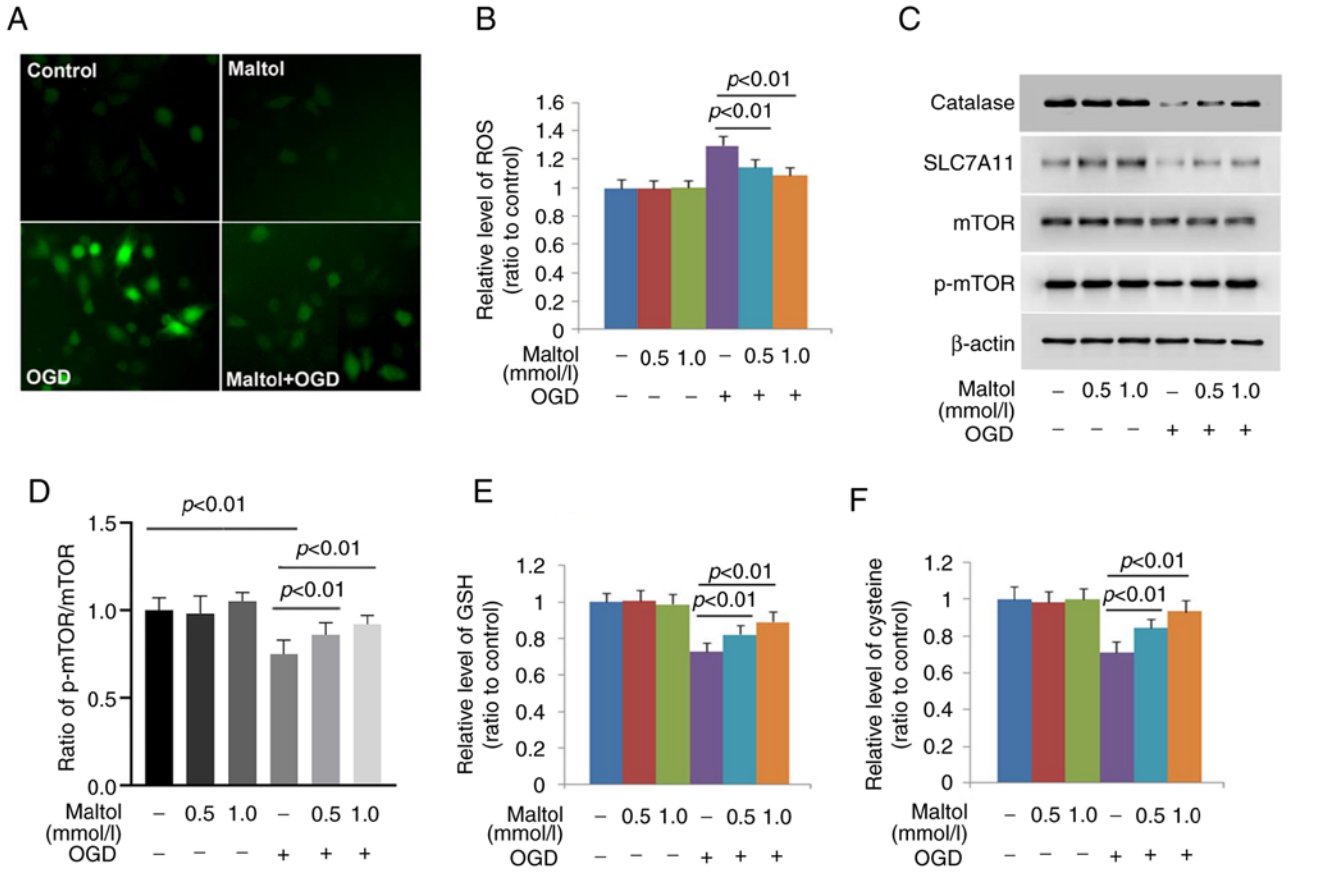

Figure 3. Maltol inhibits OGD-induced accumulation of ROS. (A) Fluorescence microscopy combined with DCFH-DA staining showed that the green fluorescence exhibited by OGD-stress cells was markedly brighter than that in control cells, but was inhibited when the cells were pretreated with maltol. (B) Statistical analysis of the fluorescence intensity demonstrated that maltol inhibited OGD-induced ROS in a dose-dependent manner. (C) Western blotting revealed that maltol apparently prevented OGD-induced downregulation of catalase, SLC7A11 and p-mTOR. (D) Statistical analysis demonstrated that the ratio of p-mTOR/mTOR in mitochondria was obviously decreased by OGD, which could be prevented by maltol. (E and F) Maltol prevented OGD-triggered depletion of GSH and cysteine. OGD, oxygen and glucose deprivation; ROS, reactive oxygen species; p-, phosphorylated.

ROS via two pathways; one was inhibiting depletion of GSH and cysteine by maintaining xCT level and the other was abrogating catalase downregulation. In addition, it was identified that maltol alleviated OGD-induced mTOR inactivation via inhibiting pyruvate depletion. Considering that activated mTOR could promote xCT expression and inhibit catalase degradation by autophagy, the present data suggested that ROS-dependent chromatinolysis induced by OGD was inhibited by maltol via preventing glycolysis dysfunction-dependent inactivation of mTOR.

As a crucial step leading to cell death, chromatinolysis is involved in regulation of apoptosis and necroptosis. It was reported that it not only contributes to staurosporine-induced apoptosis in Jurkat cells, but also regulates shikonin-triggered glioma cell necroptosis (5,31). DNA was cleaved into fragments of ~180-200 bp by activated endonucleases such as caspase-activated DNase and endonuclease G during the process of apoptosis (5), but was cleaved randomly under the condition of necroptosis (5). This explains why the nuclear DNA extracted from necroptotic cells presents continuous smear bands after electrophoresis on agarose gel, whereas the DNA extracted from apoptotic ones displays ladder bands (5). It was reported that both brain ischemia and OGD induce neuronal death via necroptosis; despite that, it remains elusive whether chromatinolysis plays a role during the process of neuronal death caused by brain ischemia or OGD (32,33). Previously, it was reported that OGD could induce damages in mitochondria, endoplasmic reticulum and disrupt in cell membrane (34-36). In the present study, it was identified that OGD could induce chromatinolysis given that the nuclear DNA extracted from the cells stressed by OGD presented smear band on agarose gel. By contrast, pretreatment with maltol obviously inhibited the smear band. Thus, maltol protected SH-SY5Y cells against OGD stress via inhibition of chromatinolysis.

Nuclear translocation of AIF from mitochondria is a crucial event causing chromatinolysis in both apoptotic and necroptotic cells (2,31). Within nuclei, AIF is recruited to λ-H2AX on damaged DNA and performs as a nuclease to degrade DNA (2). It is also required for nuclear recruitment of macrophage migration inhibitory factor (MIF), which exacerbates chromatinolysis via cleaving genomic DNA into large fragments (37). Either cerebral ischemia or OGD was reported to induce neuronal damage via causing AIF translocation from mitochondria to nuclei (38,39). Further study showed that activated JNK could exacerbate cerebral ischemia-induced mitochondrial depolarization by translocation to mitochondria (26). Different with previous reports showing that ginsenoside Rb1 and baicalein exerted protection on neuronal mitochondria against ischemic insults (38,39), maltol could enhance PINK1/Parkin-mediated autophagic

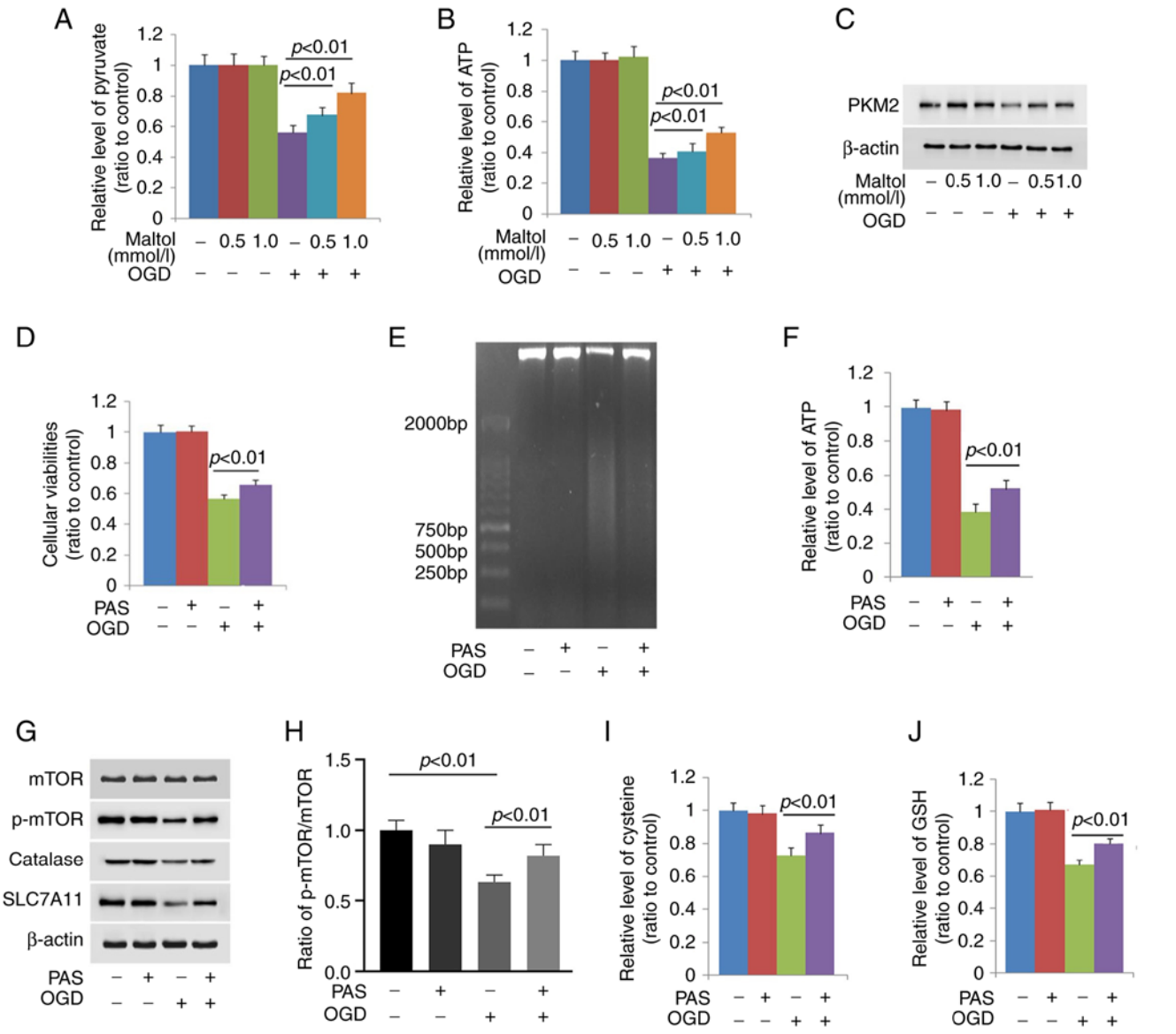

Figure 4. Maltol maintains pyruvate level. (A) Maltol inhibited OGD-induced depletion of pyruvate. (B) Maltol prevented OGD-induced reduction of ATP. (C) Western blotting showed that maltol inhibited OGD-induced downregulation of PKM2. (D) MTT assay showed that pretreatment with PAS significantly prevented OGD-induced reduction in the viabilities of SH-SY5Y cells. (E) The smear band exhibited by the nuclear DNA extracted from OGD-stressed cells on agarose gel was apparently inhibited by pretreatment with PAS. (F) Supplement of exterior PAS restored OGD-induced reduction of ATP. (G) Western blotting showed that supplement of exterior PAS restored OGD-induced downregulation of catalase, SLC7A11 and p-mTOR. (H) Statistical analysis demonstrated that the ratio of p-mTOR/mTOR was obviously decreased by OGD, which could be prevented by PAS. (I and J) Supplement of exterior PAS restored OGD-induced reduction of GSH and cysteine. OGD, oxygen and glucose deprivation; PAS, pyruvate sodium; p-, phosphorylated.

removal of damaged mitochondria (33). The data of the present study proved that maltol effectively inhibited OGD-induced mitochondria depolarization, nuclear translocation of AIF and mitochondrial accumulation of p-JNK. Thus, maltol prevented OGD-induced nuclear translocation of AIF by inhibition of JNK activation, which further attenuated OGD-induced chromatinolysis.

DNA DSBs is another factor leading to chromatinolysis. Upon occurrence of DNA DSBs, ATM is activated and then generates λ-H2AX which could serve as a platform to recruit nucleases (40). It has been reported that both cerebral ischemia and OGD could trigger DNA DSBs in neuron (41-43). Besides ion radiation, ROS are regarded as a crucial factor leading to DNA DSBs because bioactive macromolecules including proteins, lipids and nucleic acids are easily attacked by ROS (44). Moreover, ROS is a common pathological feature of cerebral ischemia, traumatic brain injury and epilepsy (44). Previous studies showed that pretreatment with maltol could effectively rescue hydrogen peroxide-induced death in human SH-SY5Y cells and rat retinal neuronal cells (45,46). In the present study, it was found that maltol markedly prevented OGD-induced λ-H2AX formation and phosphorylation of ATM, as well as effectively inhibited ROS accumulation. Another study revealed that maltol not only upregulates the expression of Nrf2, but also promotes its translocation into nuclei (12). Within nuclei, Nrf2 acts as a transcription factor accounting for upregulating the expression of inducible antioxidant enzymes (47). Thus, inhibition of ROS-dependent DNA DSBs is the other pathway via which maltol prevented OGD-induced chromatinolysis.

ROS resulting from disrupted balance between their generation and clearance could lead to DNA DSBs and nuclear translocation of AIF (6). The ROS induced by transient ischemia or GOD was closely associated with downregulation of catalase and depletion of GSH (48-50). Dioscin attenuated OGD-induced oxidative stress in hippocampal neurons via reversing catalase downregulation and GSH depletion (49). Cysteine that is converted from cystine appears to play a crucial role in regulation of intracellular ROS levels. A previous study showed that cysteine exerts inhibitory effect on intracellular H_2O_2 via two pathways. One is to be used for synthesizing GSH which is then used by GPX4 to reduce H_2O_2, and the other is to inhibit superoxide generation by mitochondrial complex III (51). In the present study, it was identified that OGD induced downregulation of catalase and depletion of GSH and cysteine in SH-SY5Y cells, which were all significantly prevented by pretreatment with maltol. Therefore, maltol prevented OGD-induced ROS via maintaining GSH and cysteine levels.

Downregulation of SLC7A11 is a pathway via which ischemia improves neuronal ROS levels (52). It was found that inhibition of SLC7A11 resulted in ROS accumulation by depletion of GSH and cysteine. As a specific inhibitor of SLC7A11, erastin was reported to induce death in primary spinal cord neurons via improving intracellular ROS (53). Previous studies showed that the protein level of SLC7A11 could be regulated by p53 and mTOR, both of which play opposite role in regulation of SLC7A11 expression. Activated p53 could suppress SLC7A11 expression directly, but activated mTOR upregulates SLC7A11 at transcriptional level via mediating Oct1 signaling (54). Because catalase and Δ133p53 (an inhibitor of full-length p53) are both selective substrates of autophagy, mTOR inactivation could promote catalase removal and p53 activation via autophagic pathway (55). Thus, mTOR inactivation exacerbates downregulation of SLC7A11 and catalase. In the present study, it was found that maltol obviously restored OGD-induced mTOR inactivation. Consistently, another study showed as well that maltol not only could restore mTOR activity via the PI3K/Akt pathway, but also could inhibit p53 activation (56). Thus, maltol prevented OGD-induced downregulation of SLC7A11 and catalase via maintaining mTOR activity.

mTOR signaling is often inactivated upon lack of energy supply (54). Previous studies showed that pyruvate plays an important role in regulating mTOR activity. After being produced primarily by glycolysis, pyruvate enters into tricarboxylic acid cycle and then is used to generate ATP to supply energy (57). Additionally, pyruvate is also an interior ROS scavenger, which is supported by the finding that pyruvate effectively protected neuronal cells against challenge by hydrogen peroxide (58). Thus, pyruvate depletion could lead to energy failure and oxidative stress, both of which could inactivate mTOR. Reversely, mTOR inactivation could result in pyruvate depletion. It was recently reported that suppression of mTOR by deoxy-shikonin inhibited glycolysis and depleted pyruvate in acute myeloid leukemia cells (59). Therefore, pyruvate depletion and mTOR inactivation could exacerbate mutually. In the present study, it was identified that supplement of exterior pyruvate not only inhibited OGD-induced ATP depletion, but also prevented p-mTOR downregulation. Correspondingly, the downregulated catalase and SLC7A11 and the depleted GSH and cysteine were all abrogated by exterior pyruvate. Thus, pyruvate depletion due to glycolysis dysfunction contributed to OGD-induced inactivation of mTOR. Notably, maltol significantly prevented OGD-triggered depletion of pyruvate. Thus, maltol maintained pyruvate level in the cells stressed by OGD.

In conclusion, the present study demonstrated that maltol effectively inhibited OGD-induced chromatinolysis via maintaining pyruvate level in SH-SY5Y cells and may be a potential medicine for cerebral ischemia.

Acknowledgements

Not applicable.

Funding

The present study was supported by the National Nature and Science Foundation of China (grant nos. 81972346 and 82173027), the Scientific Research Foundation of Jilin (grant no. 20200201405JC), the Achievement Transformation Fund of the First Hospital of Jilin University (grant no. CGZHYD202012-028) and the Development and Reform Fund of Jilin (grant no. 2014G074).

Availability of data and materials

The datasets used and/or analyzed during the current study are available from the corresponding author on reasonable request.

Authors' contributions

SZ conceptualized the study and provided methodology. XZ provided resources and performed visualization. XW conducted investigation, prepared the original draft and wrote the manuscript. CL conducted investigation. XZ, CH and TL performed validation, formal analysis and data curation. TL conducted validation and visualization. PG conceptualized and supervised the study, performed visualization, wrote, reviewed and edited the manuscript. All authors read and approved the final manuscript. SZ and PG confirm the authenticity of all the raw data.

Ethics approval and consent to participate

Not applicable.

Patient consent for publication

Not applicable.

Competing interests

The authors declare that they have no competing interests.

References

1. Kawane K, Motani K and Nagata S: DNA degradation and its defects. Cold Spring Harb Perspect Biol 6: a016394, 2014.
2. Artus C, Boujrad H, Bouharrour A, Brunelle MN, Hoos S, Yuste VJ, Lenormand P, Rousselle JC, Namane A, England P, *et al*: AIF promotes chromatinolysis and caspase-independent programmed necrosis by interacting with histone H2AX. Embo J 29: 1585-1599, 2010.

3. Baritaud M, Cabon L, Delavallée L, Galán-Malo P, Gilles ME, Brunelle-Navas MN and Susin SA: AIF-mediated caspase-independent necroptosis requires ATM and DNA-PK-induced histone H2AX Ser139 phosphorylation. Cell Death Dis 3: e390, 2012.
4. Pilch DR, Sedelnikova OA, Redon C, Celeste A, Nussenzweig A and Bonner WM: Characteristics of gamma-H2AX foci at DNA double-strand breaks sites. Biochem Cell Biol 81: 123-129, 2003.
5. Ding Y, He C, Lu S, Wang X, Wang C, Wang L, Zhang J, Piao M, Chi G, Luo Y, *et al*: MLKL contributes to shikonin-induced glioma cell necroptosis via promotion of chromatinolysis. Cancer Lett 467: 58-71, 2019.
6. He C, Lu S, Wang XZ, Wang CC, Wang L, Liang SP, Luo TF, Wang ZC, Piao MH, Chi GF and Ge PF: FOXO3a protects glioma cells against temozolomide-induced DNA double strand breaks via promotion of BNIP3-mediated mitophagy. Acta Pharmacol Sin 42: 1324-1337, 2021.
7. Berdelle N, Nikolova T, Quiros S, Efferth T and Kaina B: Artesunate induces oxidative DNA damage, sustained DNA double-strand breaks, and the ATM/ATR damage response in cancer cells. Mol Cancer Ther 10: 2224-2233, 2011.
8. Han Y, Xu Q, Hu JN, Han XY, Li W and Zhao LC: Maltol, a food flavoring agent, attenuates acute alcohol-induced oxidative damage in mice. Nutrients 7: 682-696, 2015.
9. Murakami K, Ishida K, Watakabe K, Tsubouchi R, Haneda M and Yoshino M: Prooxidant action of maltol: Role of transition metals in the generation of reactive oxygen species and enhanced formation of 8-hydroxy-2'-deoxyguanosine formation in DNA. Biometals 19: 253-257, 2006.
10. Liu W, Wang Z, Hou JG, Zhou YD, He YF, Jiang S, Wang YP, Ren S and Li W: The liver protection effects of maltol, a flavoring agent, on carbon tetrachloride-induced acute liver injury in mice via inhibiting apoptosis and inflammatory response. Molecules 23: 2120, 2018.
11. Wang Z, Hao W, Hu J, Mi X, Han Y, Ren S, Jiang S, Wang Y, Li X and Li W: Maltol Improves APAP-Induced hepatotoxicity by inhibiting oxidative stress and inflammation response via NF-κB and PI3K/Akt signal pathways. Antioxidants (Basel) 8: 395, 2019.
12. Zhu DC, Wang YH, Lin JH, Miao ZM, Xu JJ and Wu YS: Maltol inhibits the progression of osteoarthritis via the nuclear factor-erythroid 2-related factor-2/heme oxygenase-1 signal pathway in vitro and in vivo. Food Funct 12: 1327-1337, 2021.
13. Guo N, Li C, Liu Q, Liu S, Huan Y, Wang X, Bai G, Yang M, Sun S, Xu C and Shen Z: Maltol, a food flavor enhancer, attenuates diabetic peripheral neuropathy in streptozotocin-induced diabetic rats. Food Funct 9: 6287-6297, 2018.
14. Mi XJ, Hou JG, Jiang S, Liu Z, Tang S, Liu XX, Wang YP, Chen C, Wang Z and Li W: Maltol mitigates thioacetamide-induced liver fibrosis through TGF-β1-mediated activation of PI3K/Akt signaling pathway. J Agric Food Chem 67: 1392-1401, 2019.
15. Hong S, Iizuka Y, Lee T, Kim CY and Seong GJ: Neuroprotective and neurite outgrowth effects of maltol on retinal ganglion cells under oxidative stress. Mol Vis 20: 1456-1462, 2014.
16. Kim YB, Oh SH, Sok DE and Kim MR: Neuroprotective effect of maltol against oxidative stress in brain of mice challenged with kainic acid. Nutr Neurosci 7: 33-39, 2004.
17. Mao Y, Du J, Chen X, Al Mamun A, Cao L, Yang Y, Mubwandarikwa J, Zaeem M, Zhang W, Chen Y, *et al*: Maltol promotes mitophagy and inhibits oxidative stress via the Nrf2/PINK1/Parkin pathway after spinal cord injury. Oxid Med Cell Longev 2022: 1337630, 2022.
18. Badiola N, Penas C, Miñano-Molina A, Barneda-Zahonero B, Fadó R, Sánchez-Opazo G, Comella JX, Sabriá J, Zhu C, Blomgren K, *et al*: Induction of ER stress in response to oxygen-glucose deprivation of cortical cultures involves the activation of the PERK and IRE-1 pathways and of caspase-12. Cell Death Dis 2: e149, 2011.
19. Lee HJ, Lyu da H, Koo U, Lee SJ, Hong SS, Kim K, Kim KH, Lee D and Mar W: Inhibitory effect of 2-arylbenzofurans from the Mori Cortex Radicis (Moraceae) on oxygen glucose deprivation (OGD)-induced cell death of SH-SY5Y cells. Arch Pharm Res 34: 1373-1380, 2011.
20. Zhou Z, Lu B, Wang C, Wang Z, Luo T, Piao M, Meng F, Chi G, Luo Y and Ge P: RIP1 and RIP3 contribute to shikonin-induced DNA double-strand breaks in glioma cells via increase of intracellular reactive oxygen species. Cancer Lett 390: 77-90, 2017.
21. Wang C, He C, Lu S, Wang X, Wang L, Liang S, Wang X, Piao M, Cui J, Chi G and Ge P: Autophagy activated by silibinin contributes to glioma cell death via induction of oxidative stress-mediated BNIP3-dependent nuclear translocation of AIF. Cell Death Dis 11: 630, 2020.
22. Begum H, Murugesan P and Tangutur AD: Western blotting: A powerful staple in scientific and biomedical research. Biotechniques 73: 58-69, 2022.
23. Huang Y, Wen Q, Huang J, Luo M, Xiao Y, Mo R and Wang J: Manganese (II) chloride leads to dopaminergic neurotoxicity by promoting mitophagy through BNIP3-mediated oxidative stress in SH-SY5Y cells. Cell Mol Biol Lett 26: 23, 2021.
24. Wang HF, Wang ZQ, Ding Y, Piao MH, Feng CS, Chi GF, Luo YN and Ge PF: Endoplasmic reticulum stress regulates oxygen-glucose deprivation-induced parthanatos in human SH-SY5Y cells via improvement of intracellular ROS. CNS Neurosci Ther 24: 29-38, 2018.
25. Andrabi SA, Dawson TM and Dawson VL: Mitochondrial and nuclear cross talk in cell death: Parthanatos. Ann N Y Acad Sci 1147: 233-241, 2008.
26. Xia P, Zhang F, Yuan Y, Chen C, Huang Y, Li L, Wang E, Guo Q and Ye Z: ALDH 2 conferred neuroprotection on cerebral ischemic injury by alleviating mitochondria-related apoptosis through JNK/caspase-3 signing pathway. Int J Biol Sci 16: 1303-1323, 2020.
27. Ali SS, Ahsan H, Zia MK, Siddiqui T and Khan FH: Understanding oxidants and antioxidants: Classical team with new players. J Food Biochem 44: e13145, 2020.
28. Li C, Chen H, Lan Z, He S, Chen R, Wang F, Liu Z, Li K, Cheng L, Liu Y, *et al*: mTOR-dependent upregulation of xCT blocks melanin synthesis and promotes tumorigenesis. Cell Death Differ 26: 2015-2028, 2019.
29. Dey P, Kundu A, Sachan R, Park JH, Ahn MY, Yoon K, Lee J, Kim ND, Kim IS, Lee BM, *et al*: PKM2 knockdown induces autophagic cell death via AKT/mTOR pathway in human prostate cancer cells. Cell Physiol Biochem 52: 1535-1552, 2019.
30. Li XB, Gu JD and Zhou QH: Review of aerobic glycolysis and its key enzymes-new targets for lung cancer therapy. Thorac Cancer 6: 17-24, 2015.
31. Candé C, Vahsen N, Kouranti I, Schmitt E, Daugas E, Spahr C, Luban J, Kroemer RT, Giordanetto F, Garrido C, *et al*: AIF and cyclophilin A cooperate in apoptosis-associated chromatinolysis. Oncogene 23: 1514-1521, 2004.
32. Li J, Zhang J, Zhang Y, Wang Z, Song Y, Wei S, He M, You S, Jia J and Cheng J: TRAF2 protects against cerebral ischemia-induced brain injury by suppressing necroptosis. Cell Death Dis 10: 328, 2019.
33. Tang MB, Li YS, Li SH, Cheng Y, Zhang S, Luo HY, Mao CY, Hu ZW, Schisler JC, Shi CH, *et al*: Anisomycin prevents OGD-induced necroptosis by regulating the E3 ligase CHIP. Sci Rep 8: 6379, 2018.
34. Park YH, Broyles HV, He S, McGrady NR, Li L and Yorio T: Involvement of AMPA receptor and its flip and flop isoforms in retinal ganglion cell death following oxygen/glucose deprivation. Invest Ophthalmol Vis Sci 57: 508-526, 2016.
35. Li HQ, Xia SN, Xu SY, Liu PY, Gu Y, Bao XY, Xu Y and Cao X: γ-Glutamylcysteine alleviates ischemic stroke-induced neuronal apoptosis by inhibiting ROS-Mediated endoplasmic reticulum stress. Oxid Med Cell Longev 2021: 2961079, 2021.
36. Qu Y, Tang J, Wang H, Li S, Zhao F, Zhang L, Richard Lu Q and Mu D: RIPK3 interactions with MLKL and CaMKII mediate oligodendrocytes death in the developing brain. Cell Death Dis 8: e2629, 2017.
37. Wang Y, An R, Umanah GK, Park H, Nambiar K, Eacker SM, Kim B, Bao L, Harraz MM, Chang C, *et al*: A nuclease that mediates cell death induced by DNA damage and poly(ADP-ribose) polymerase-1. Science 354: aad6872, 2016.
38. Li WH, Yang YL, Cheng X, Liu M, Zhang SS, Wang YH and Du GH: Baicalein attenuates caspase-independent cells death via inhibiting PARP-1 activation and AIF nuclear translocation in cerebral ischemia/reperfusion rats. Apoptosis 25: 354-369, 2020.
39. Liang J, Yu Y, Wang B, Lu B, Zhang J, Zhang H and Ge P: Ginsenoside Rb1 attenuates oxygen-glucose deprivation-induced apoptosis in SH-SY5Y cells via protection of mitochondria and inhibition of AIF and cytochrome c release. Molecules 18: 12777-12792, 2013.
40. Lee JH and Paull TT: Cellular functions of the protein kinase ATM and their relevance to human disease. Nat Rev Mol Cell Biol 22: 796-814, 2021.
41. Sánchez-Morán I, Rodríguez C, Lapresa R, Agulla J, Sobrino T, Castillo J, Bolaños JP and Almeida A: Nuclear WRAP53 promotes neuronal survival and functional recovery after stroke. Sci Adv 6: eabc5702, 2020.

42. Cheng J, Fan YQ, Jiang HX, Chen SF, Chen J, Liao XY, Zou YY, Lan HY, Cui Y, Chen ZB, *et al*: Transcranial direct-current stimulation protects against cerebral ischemia-reperfusion injury through regulating Cezanne-dependent signaling. Exp Neurol 345: 113818, 2021.
43. Kihara S, Shiraishi T, Nakagawa S, Toda K and Tabuchi K: Visualization of DNA double strand breaks in the gerbil hippocampal CA1 following transient ischemia. Neurosci Lett 175: 133-136, 1994.
44. Floyd RA and Carney JM: Free radical damage to protein and DNA: Mechanisms involved and relevant observations on brain undergoing oxidative stress. Ann Neurol 32 (Suppl 1): S22-S27, 1992.
45. Yang Y, Wang J, Xu C, Pan H and Zhang Z: Maltol inhibits apoptosis of human neuroblastoma cells induced by hydrogen peroxide. J Biochem Mol Biol 39: 145-149, 2006.
46. Song Y, Hong S, Iizuka Y, Kim CY and Seong GJ: The neuroprotective effect of maltol against oxidative stress on rat retinal neuronal cells. Korean J Ophthalmol 29: 58-65, 2015.
47. Zhang H, Davies KJA and Forman HJ: Oxidative stress response and Nrf2 signaling in aging. Free Radic Biol Med 88: 314-336, 2015.
48. Dai Y, Zhang H, Zhang J and Yan M: Isoquercetin attenuates oxidative stress and neuronal apoptosis after ischemia/reperfusion injury via Nrf2-mediated inhibition of the NOX4/ROS/NF-κB pathway. Chem Biol Interact 284: 32-40, 2018.
49. Liu A, Zhang W, Wang S, Wang Y and Hong J: HMGB-1/RAGE signaling inhibition by dioscin attenuates hippocampal neuron damage induced by oxygen-glucose deprivation/reperfusion. Exp Ther Med 20: 231, 2020.
50. Armogida M, Spalloni A, Amantea D, Nutini M, Petrelli F, Longone P, Bagetta G, Nisticò R and Mercuri NB: The protective role of catalase against cerebral ischemia in vitro and in vivo. Int J Immunopathol Pharmacol 24: 735-747, 2011.
51. Rhee SG and Kil IS: Mitochondrial H_2O_2 signaling is controlled by the concerted action of peroxiredoxin III and sulfiredoxin: Linking mitochondrial function to circadian rhythm. Free Radic Biol Med 99: 120-127, 2016.
52. Fu C, Wu Y, Liu S, Luo C, Lu Y, Liu M, Wang L, Zhang Y and Liu X: Rehmannioside A improves cognitive impairment and alleviates ferroptosis via activating PI3K/AKT/Nrf2 and SLC7A11/GPX4 signaling pathway after ischemia. J Ethnopharmacol 289: 115021, 2022.
53. Wei N, Lu T, Yang L, Dong Y and Liu X: Lipoxin A4 protects primary spinal cord neurons from Erastin-induced ferroptosis by activating the Akt/Nrf2/HO-1 signaling pathway. FEBS Open Bio 11: 2118-2126, 2021.
54. Woo Y, Lee HJ, Kim J, Kang SG, Moon S, Han JA, Jung YM and Jung YJ: Rapamycin Promotes ROS-Mediated cell death via functional inhibition of xCT Expression in Melanoma Under γ-Irradiation. Front Oncol 11: 665420, 2021.
55. Horikawa I, Fujita K, Jenkins LM, Hiyoshi Y, Mondal AM, Vojtesek B, Lane DP, Appella E and Harris CC: Autophagic degradation of the inhibitory p53 isoform Δ133p53α as a regulatory mechanism for p53-mediated senescence. Nat Commun 5: 4706, 2014.
56. Mi XJ, Hou JG, Wang Z, Han Y, Ren S, Hu JN, Chen C and Li W: The protective effects of maltol on cisplatin-induced nephrotoxicity through the AMPK-mediated PI3K/Akt and p53 signaling pathways. Sci Rep 8: 15922, 2018.
57. Wang X, Perez E, Liu R, Yan LJ, Mallet RT and Yang SH: Pyruvate protects mitochondria from oxidative stress in human neuroblastoma SK-N-SH cells. Brain Res 1132: 1-9, 2007.
58. Zeng J, Yang GY, Ying W, Kelly M, Hirai K, James TL, Swanson RA and Litt L: Pyruvate improves recovery after PARP-1-associated energy failure induced by oxidative stress in neonatal rat cerebrocortical slices. J Cereb Blood Flow Metab 27: 304-315, 2007.
59. Wu H, Zhao H and Chen L: Deoxyshikonin inhibits viability and glycolysis by suppressing the Akt/mTOR pathway in acute myeloid leukemia cells. Front Oncol 10: 1253, 2020.